Check for updates

Dynamic Diatom-Bacteria Consortia in Synthetic Plankton Communities

Yun Deng,[a] Marco Mauri,[b,c] Marine Vallet,[d] Mona Staudinger,[a] Rosalind J. Allen,[b,c] Georg Pohnert[a,d]

[a]Institute for Inorganic and Analytical Chemistry, Friedrich Schiller University Jena, Jena, Germany
[b]Theoretical Microbial Ecology Group, Institute of Microbiology, Faculty of Biological Sciences, Friedrich Schiller University Jena, Jena, Germany
[c]School of Physics and Astronomy, University of Edinburgh, Edinburgh, United Kingdom
[d]Phytoplankton Community Interactions Research Group, Max Planck Institute for Chemical Ecology, Jena, Germany

ABSTRACT Microalgae that form phytoplankton live and die in a complex microbial consortium in which they co-exist with bacteria and other microorganisms. The dynamics of species succession in the plankton depends on the interplay of these partners. Bacteria utilize substrates produced by the phototrophic algae, while algal growth can be supported by bacterial exudates. Bacteria might also use chemical mediators with algicidal properties to attack algae. To elucidate whether specific bacteria play universal or context-specific roles in the interaction with phytoplankton, we investigated the effect of cocultured bacteria on the growth of 8 microalgae. An interaction matrix revealed that the function of a given bacterium is highly dependent on the cocultured partner. We observed no universally algicidal or universally growth-promoting bacteria. The activity of bacteria can even change during the aging of an algal culture from inhibitory to stimulatory or vice versa. We further established a synthetic phytoplankton/bacteria community with the centric diatom, *Coscinodiscus radiatus*, and 4 phylogenetically distinctive bacterial isolates, *Mameliella* sp., *Roseovarius* sp., *Croceibacter* sp., and *Marinobacter* sp. Supported by a Lotka-Volterra model, we show that interactions within the consortium are specific and that the sum of the pairwise interactions can explain algal and bacterial growth in the community. No synergistic effects between bacteria in the presence of the diatom was observed. Our survey documents highly species-specific interactions that are dependent on algal fitness, bacterial metabolism, and community composition. This species specificity may underly the high complexity of the multi-species plankton communities observed in nature.

IMPORTANCE The marine food web is fueled by phototrophic phytoplankton. These algae are central primary producers responsible for the fixation of ca. 40% of the global CO_2. Phytoplankton always co-occur with a diverse bacterial community in nature. This diversity suggests the existence of ecological niches for the associated bacteria. We show that the interaction between algae and bacteria is highly species-specific. Furthermore, both, the fitness stage of the algae and the community composition are relevant in determining the effect of bacteria on algal growth. We conclude that bacteria should not be sorted into algicidal or growth supporting categories; instead, a context-specific function of the bacteria in the plankton must be considered. This functional diversity of single players within a consortium may underly the observed diversity in the plankton.

KEYWORDS phytoplankton, microalgae, bacteria, diatoms, microbiome, consortia, interactions, host-cell interactions

A nnual phytoplankton successions determine biogeochemical element cycles. Light, temperature, and nutrients are the main drivers for seasonal successions (1). Laboratory and field surveys suggest that biological interactions between phytoplankton and its

associated bacterial microbiome influence algal development as well (2–4). Natural planktonic communities are highly complex, and their species composition is controlled by many variables. Eukaryotic and prokaryotic cells with diverse traits interact at a given time (5). Therefore, functional deductions from field work are hard to obtain and rely on modeling and correlation analysis. Studies of interactions between pairs of species in the lab do not reflect the complex situation in the ocean. This renders the elucidation of interspecies interactions challenging. Approaches based on complex coculture techniques combined with modeling of the resulting microbial communities can provide a basis to study these biological interactions. With such setups, cell-to-cell communication (6), programmed cell death (7), and stress responses (8) within communities can be identified and provide an understanding of the mechanisms controlling natural algal blooms (3).

Diatoms account for 25% of primary production globally and are widely distributed (9). Their importance and their diverse adaptation-related traits make them central players in phytoplankton community functioning (4). Heterotrophic bacteria are often associated with diatoms and act as key recyclers. The diatom-associated bacteria turn over dissolved organic matter produced from photosynthesis, and also support algal bloom development by supplying vitamins (10). Therefore, ecologically relevant studies of diatoms have to take their associated bacterial microbiome into account. Studies of one-to-one bacteria-algae interactions can provide mechanistic insight. Such studies revealed that bacteria initiate the rapid reproduction of diatoms (11), promote the formation of a persistent community (12), and accelerate the lysis of algae hosts (13, 14). A full understanding of how bacteria interact with algal hosts and affect the dynamics of the community can, however, only be obtained by investigating the microbiome in all its complexity (15, 16).

Building of complex multipartite model systems in the lab is highly challenging. The recently established tripartite laboratory community consisting of the algicidal bacterium *Kordia algicida* strain OT1, the resistant diatom *Chaetoceros didymus*, and the susceptible diatom *Skeletonema costatum* provides a model for studying the mechanism of phytoplankton community succession in the lab (14) and the field (17). In another recently established system, co-cultivation of 2 bacteria and the diatom *Phaeodactylum tricornutum* in a porous microplate enables the study of metabolic exchanges between algae and associated bacteria (18). However, the construction of more complex stable communities that would allow for studies of the effects of different bacteria on community dynamics remains challenging.

To establish a synthetic community model that allows to address ecological questions in plankton, requires selection of species based on the following considerations: (i) Ecological relevance and natural abundance, (ii) widespread taxonomic species that co-exist in their natural environment, (iii) observable traits as indicators for plankton community functioning, (iv) significant biological effects between the interacting partners, and, whenever possible, (v) genetic support and engineering possibilities.

Here, we integrated these considerations into an effects-driven screening procedure to build model communities composed of bacteria and algae. We initially screened for bacteria-algae interactions and then selected the microbial partners for the construction of a synthetic planktonic community. A two species coculturing was used to characterize the mode of interactions before transferring the partners into a more complex community. Mathematical modeling was used to interpret the population dynamics data for diatom-bacterial cocultures. We thereby identified multiple factors including species composition, fitness, and community structure influencing the composition and performance of the plankton microbiome.

RESULTS

Screening of bilateral interactions between phytoplankton and bacteria. Eight widely distributed, ecologically relevant diatoms were included in an initial screen for growth-promoting or inhibiting effects of 16 different bacteria (Fig. 1a, Fig. S1, and Table S1). Cell phenotypes, including size and shape were diverse, with *Coscinodiscus*
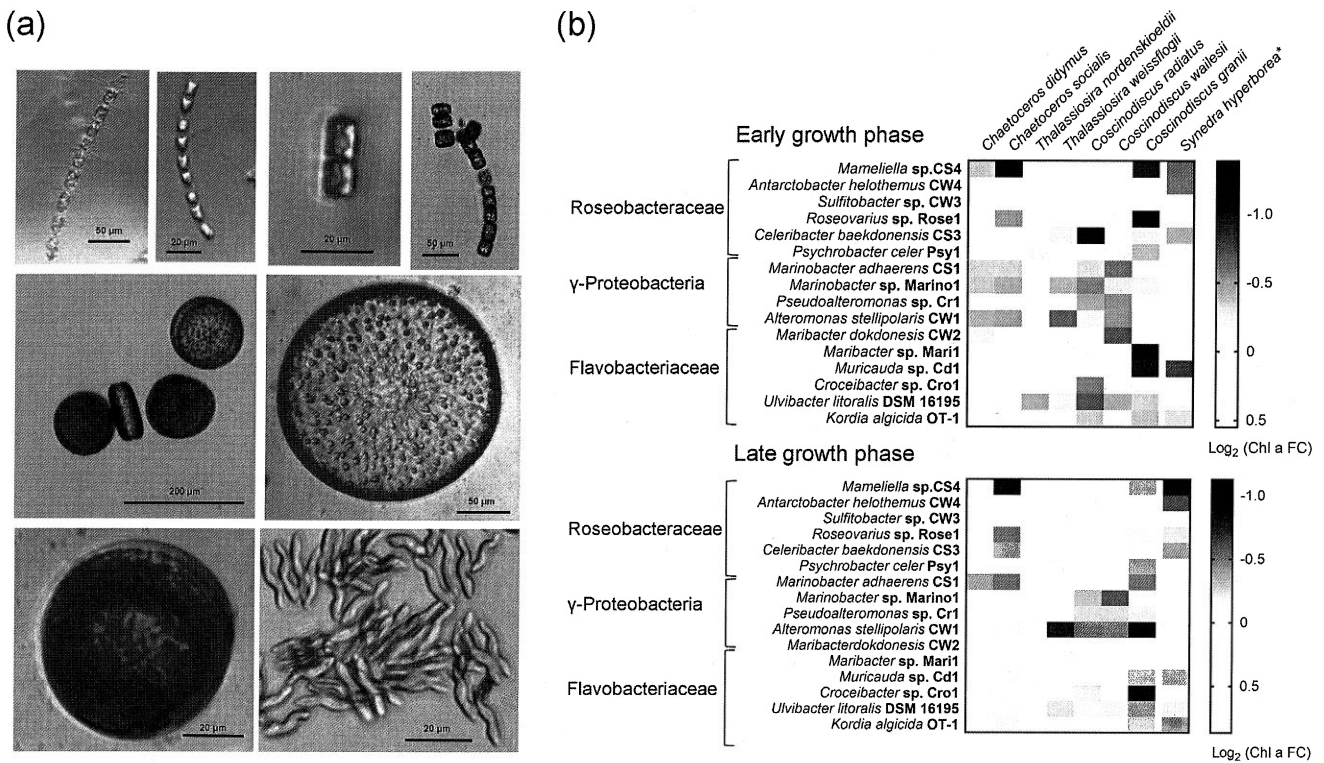
(a)

(b)

FIG 1 Pairwise co-cultivation to identify interaction patterns between bacteria and diatoms. (a) Cell morphology of the 8 diatoms used in this study. Clockwise from the top left: *C. didymus, C. socialis, T. weissflogii, T. nordenskioeldii, C. wailesii, S. hyperborea, C. granii,* and *C. radiatus*. (b) Heatmaps summarize the effects of bacteria on diatoms in their early (before reaching the chlorophyll maximum) and late (after reaching the chlorophyll maximum) growth phase. The workflow for plotting the heatmaps is described in Fig. S2. Average of *n* = 3 replicates is plotted, growth curves for each pairwise interaction are given in Fig. S3-S10. *Data were normalized by the average cell densities determined for all cocultures with different bacterial inoculations. Chla FC refers to Chlorophyll a fold change.

spp. being the largest diatom in our screening (Fig. 1a). A total of 16 bacterial strains were isolated from algal cultures and taxonomically identified based on 16S rDNA sequencing (Fig. S1b and Table S2). We focused on abundant players of the marine bacterioplankton, including 5 bacteria from the newly proposed family Roseobacteraceae (19), 5 Gammaproteobacteria, and 6 strains belonging to the Flavobacteriaceae (20). Diatoms and bacteria were co-cultivated pairwise in 48 well plates and monitoring of Chlorophyll a (Chl a) was used as a proxy for diatom growth (Fig. S2).

Bacteria have diverse effects on diatoms in the early and late growth phase. Of the 256 pairwise interactions observed, similar numbers of cases where bacteria promote or inhibit diatoms were found. However, the effect was variable during the different algal growth phases. In the early growth phase, 41% of the diatoms in pairwise interactions with bacteria were reduced in growth by a factor of 0.75 and less, while 19% were promoted in growth by a factor of 1.25 or more. In the late growth phase, promotion of survival was more pronounced with higher chlorophyll readings in 47% (> factor 1.25). Only 19% were inhibited (< 0.75) (Fig. 1b).

Strikingly, none of the tested bacteria universally promoted or inhibited growth of the different algae. The only exception was *Maribacter* sp. that had a positive effect on the performance of all diatoms in the late growth phase. The effect of a given bacterium is thus strongly dependent on the interaction partner. If the data are regarded from the algal's perspective a similar diversity of effects can be observed. In most cases, algal growth could be either promoted or inhibited, depending on the cocultured bacterium. Some diatoms, such as *Chaetoceros socialis*, rather generally perform worse in the presence of bacteria (81.3%), while others, such as *Thalassiosira nordenskioeldii*, grew better in most cocultures compared to the control (78.1%) (Fig. 1b).

In most cases the effect of a given bacterium on a diatom was consistent throughout

the algal growth phases (Fig. 1b). However, we observed several cases where growth promotion or inhibition depended on the physiological state of the diatom (all growth curves are found in Fig. S3 to S10). This was most pronounced for the interaction of *Coscinodiscus granii* with *Croceibacter* sp., where growth in the early phase was strongly promoted, while survival in the late growth phase was substantially reduced (Fig. S4).

Some patterns correlated with bacterial taxonomic groups. All the selected Gammaproteobacteria showed negative effects on *Coscinodiscus radiatus* during the early growth phase and all the investigated Roseobacteraceae showed positive effects on *C. radiatus* during the late growth phase (Fig. 1b).

Building a synthetic community of *C. radiatus* and four bacteria. In nature, bilateral interactions between bacteria and algae are likely an exception since plankton communities are highly complex with multiple co-occurring species. We, thus, set out to investigate if the properties of certain bacteria dominate in a model community or if effects are rather additive. Therefore, a coculture of 4 bacteria and one diatom was established. Based on results from the initial screening, we selected *C. radiatus* as the algal partner. This diatom has a large cell size with diameters over 100 μm. Its unique morphology offers an advantage for studying chemically mediated interactions through microscopy and mass spectrometry imaging (21). Two representative bacteria from the Roseobacteraceae family *Mameliella* CS4 (hereafter CS4) and *Roseovarius* sp. Rose1 (Rose1), a gamma-proteobacterium *Marinobacter* sp. CS1 (CS1) and the Flavobacterium *Croceibacter atlanticus* Crocei1 (Crocei1) were used in cocultures. We explicitly used comparably low bacterial cell counts and a medium poor in organic nutrients, that is based on natural seawater to mimic the situation in the surface waters. There, similarly low bacterial cell densities are observed. We aimed to reach initial densities around 5×10^5 cells/mL, which are, on average, observed in surface seawater (22).

All bacteria were initially investigated in bilateral cocultures with the diatom. Next, an artificial community was studied comprising all bacterial partners together with the diatom. Monocultures of the axenic alga and cultures of the respective bacteria were used as controls. The algal performance was evaluated by counting cells under the microscope and recording the Chl a fluorescence. Healthy and dead cells were distinguished visually based on their pigmentation (Fig. S11). Bacterial abundance was determined by qPCR (Cq values were calibrated with bacterial cells for each strain) (Fig. S12).

In all pairwise inoculations, the effects caused by bacteria were consistent with results from the screening (Fig. 1b and Fig. 2). Both bacteria from the Roseobacteraceae family (CS4 and Rose1) prolonged the stationary phase of the alga (Fig. 2b and c). Consistently, a reduced number of dead algal cells in the later stages of the coculture was observed (Fig. S13). The bacterium Crocei1 inhibited growth of the diatom throughout all growth phases (Fig. 2d). In agreement with this observation, the number of dead algal cells was higher in the coculture from day 13 onwards (Fig. S13c). The gamma-proteobacterium CS1 had a more complex effect on the growth of *C. radiatus*. It inhibited growth of the alga only during the early growth phase. Until day 9, very low algal cell numbers were recorded, but the alga then recovered to reach a similar cell density as the control (Fig. 2e).

Bacterial proliferation was affected differently by the algae (Fig. 3). The gamma-proteobacterium CS1 grew well in the medium in the absence of diatoms, possibly utilizing the 5 mM HEPES buffer in ASW2 medium that represents the only carbon source in the medium (Fig. 3e). However, the growth of CS1 was inhibited by the diatom *C. radiatus* under coculture conditions after day 9 (significant from day 11 to 21) (Fig. 3e). The diatom had no significant influence on the growth of Rose1 and CS4 (Fig. 3b and c). These bacteria grew only to low cell counts in the ASW2 medium in accordance with the poor nutrient content of the medium that is derived from natural seawater. Crocei1 grew to significantly higher density in cocultures compared to monocultures in the ASW2 medium, where it performed only poorly (Fig. 3d).

In the synthetic community of the diatom and all 4 bacteria, an inhibitory effect of the bacteria on the alga was apparent throughout the culturing phase, as shown by reduced cell counts (Fig. 2f). The most pronounced inhibition was observed from the
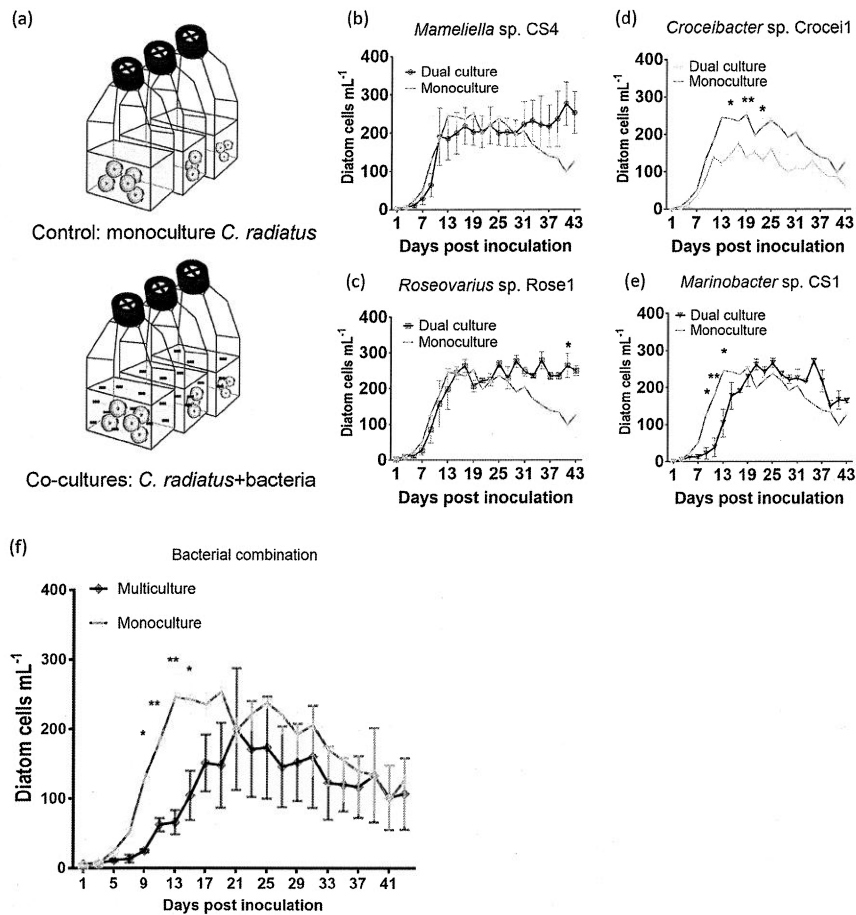
FIG 2 Cell counts in the co-cultivation of the diatom *C. radiatus* with the individual bacterial species, *Roseovarius* Rose1, *Croceibacter* Crocei1, *Marinobacter* CS1 and 4 bacteria in combination. (a) Scheme for the coculture experiment design, monoculture *C. radiatus* (upper) and *C. radiatus*-bacteria coculture (lower). Live cell counts of *C. radiatus* in coculture with the bacteria CS4 (b), Rose1(c), Crocei1(d), CS1(e) and in controls without added bacteria (orange). The effect of the coculture of the synthetic community with four bacteria combination is shown in (f). Bars derive from SE of three biological replicates. Unpaired *t* test, ** indicates $P < 0.01$, * indicates $P < 0.05$.

beginning of the culturing to day 17, but in the later growth stages the diatom cell counts of the coculture were also lower than those of the control. The slightly elevated cell counts in the very late stages of the cultures goes with reduced dead cells in the coculture (Fig. S13e). In the community, all bacteria performed similarly or slightly better compared to the monocultures and the pairwise algal-bacterial cocultures (Fig. 3f).

A generalized Lotka-Volterra model can predict the composition of the synthetic community. We developed a mathematical model to interpret our data on algal and bacterial growth in mono- and cocultures (Fig. 2, Fig. 3, Fig. S14, and Fig. S15). The generalized Lotka-Volterra model described in the Methods section predicts the dynamics of a multispecies community, taking into account pairwise interactions between species (23). Each pairwise interaction is quantified by an interaction parameter, the sign of which (positive or negative) determines whether a stimulatory or an inhibitory interaction is described (24). Additional parameters describe the growth of each species in the absence of interactions.

Using only parameters obtained from fitting the isolated cultures and the pairwise cocultures, the model correctly predicts a net inhibition of the alga by the bacterial community, with the quantitative prediction for the algal cell density being in good agreement with our data (Fig. 4b). Capturing the algal-bacterial interactions is important to obtain this agreement; a neutral model that does not consider any interspecies interactions is not in quantitative agreement with the data (Fig. S16, magenta line).
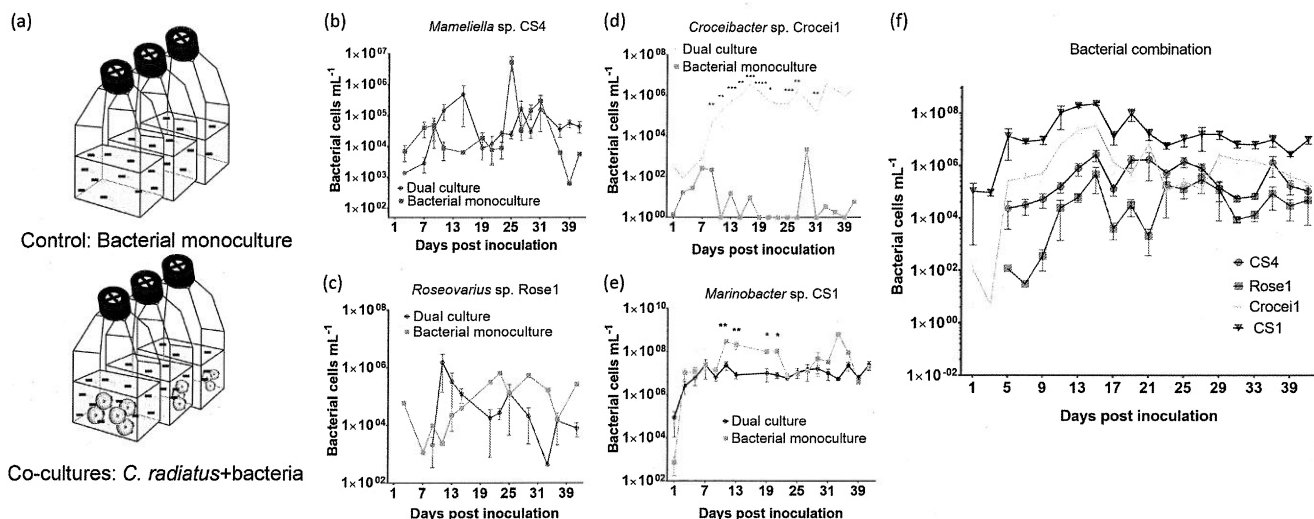
FIG 3 Bacterial quantification in the co-cultivation of the diatom *C. radiatus* with the individual bacteria, *Roseovarius* Rose1, *Croceibacter* Crocei1, *Marinobacter* CS1 and four bacteria in combination. (a) Scheme for the coculture experiment design, bacterial monoculture (upper) and *C. radiatus*-bacteria coculture (lower). Bacterial density was quantified by qPCR when initially inoculated with bacterial strains CS4 (b), Rose1(c), Crocei1(d), CS1(e) and 4 bacteria in combination (f). Controls without added diatoms are coded with gray. Bacterial cells mL^{-1} are plotted on a logarithmic scale. Bars derive from SE of three biological replicates. Unpaired *t* test, **** indicates $P < 0.001$, *** indicates $P < 0.005$, ** indicates $P < 0.01$, * indicates $P < 0.05$.

The fact that the mathematical model agrees well with the data hints that pairwise interactions might be sufficient to explain complex community behavior and high order interactions among bacteria are negligible. The analysis of the pairwise interaction parameters from the model (Fig. 4b) showed that the strongest interactions are between the bacterium Crocei1 and the alga: Crocei1 inhibits algal growth while the alga promotes the growth of Crocei1. A simpler model that only considers the strongest alga-Crocei1 interaction and the effect of CS1 in shifting the initial growth of the alga, is indeed enough to recapitulate the experimental data (plot not shown).

Auxotrophy and nutrient requirements of the tested bacteria. Auxotrophy, an organism's requirement for an exogenous source of organic molecules, can contribute to the stability of the plankton microbial community (25). A nutrient currency exchange shapes interactions between algae and bacteria. This process can be mediated by the supply of bacterial vitamins or amino acids in exchange for algal organic nutrients. To elucidate the potential for auxotrophic interactions in our synthetic community, we sequenced the genomes of the four bacteria. Genomic features of the four strains are shown in Table
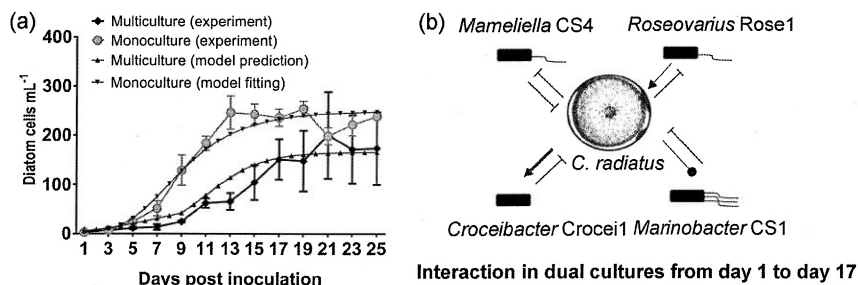

FIG 4 (a) Prediction of the mathematical Lotka-Volterra model for algal growth in the presence of all four bacteria. The black line shows the model prediction using parameters obtained by fitting to the data from isolated cultures and pairwise cocultures. The model agrees well with the experimental data (blue line). For comparison, we plotted also the data for diatom growth in isolation (orange line) and the corresponding model fit (red line). (b) Illustration of the inter-species interactions obtained from the model fit of the pairwise coculture data. Neutral, stimulatory, and inhibitory interactions are indicated by blue circle-headed, red flat and green pointed arrows, respectively. The strongest interaction detected by the model is stimulation of Crocei1 by *C. radiatus*.

TABLE 1 Predicted auxotrophies from the genomes of the four tested bacterial strains[a]

No.	*Mameliella* CS4	*Roseovarius* Rose1	*Croceibacter* Crocei1	*Marinobacter* CS1
1	L-Lysine	L-Lysine	L-Lysine	L-Lysine
2	L-Arginine	-	L-Arginine	L-Arginine
3	-	-	L-Methionine	-
4	-	L-Cysteine	L-Cysteine	-
5	L-Leucine	L-Leucine	L-Leucine	L-Leucine
6	-	-	L-Proline	-
7	-	-	L-Asparagine	-
8	-	-	L-Valine	-
9	L-Isoleucine	L-Isoleucine	L-Isoleucine	L-Isoleucine
10	-	Niacin (VB3)	-	-
11	-	-	S-adenosyl-L-methionine	-
12	-	-	Putrescine	-
13	-	-	Spermidine	-
14	-	-	VB12	VB12

[a]-, not detected.

S5. We performed an auxotrophy prediction using the 4 bacterial genomes to access their potential abilities to produce amino acids and vitamins. Of the 4 bacteria, *Croceibacter* showed the highest requirement for externally supplied amino acids and vitamins. This is also reflected by its lack of growth in ASW2 medium. Rose1 showed a deficiency in Niacin (vitamin B3, VB3) production, and all tested bacteria lack the ability to produce selected amino acids. Crocei1 and CS1 show a deficiency in vitamin 12 biosynthesis (Table 1).

Dimethylsulfoniopropionate (DMSP) is a well-studied metabolite that is primarily produced by algae and can be exploited by bacteria as a carbon and reduced sulfur source (26). DMSP metabolism can follow diverse pathways involving demethylation or cleavage (27). In the demethylation pathway, DmdA demethylates DMSP to produce 3-(methylthio)propionate (MMPA), and finally generates acetaldehyde and methanethiol under the action of the enzymes DmdB, DmdC, and DmdD. In the cleavage pathway, a DMSP lyase (DddP/L/Q/W/K/Y) converts DMSP to acrylate and dimethyl sulfide (DMS). DddD converts DMSP to 3-hydroxypropionyl-CoA and DMS. DddX converts DMSP to acryloyl-CoA and DMS. We retrieved the known protein sequences responsible for DMSP catabolism and aligned them with the predicted protein sequences from our 4 bacterial genomes via BLASTP. The proteins for the respective DMSP metabolic pathways encoded in the genomes of the 4 bacteria are listed in Table 2. CS4 and Rose1 genomes contain all genes for the demethylation and cleavage pathways. In contrast, only poorly aligned proteins for the demethylation pathway are found in Crocei 1, indicating poor or no usage of DMSP (Table 2). A crucial sequence for the demethylation pathway encoding the protein DmdA is missing in the CS1 genome, but the other proteins DmdB/C/D are present. This suggests that CS1 might metabolize the product MMPA of DMSP demethylation. These genome analyses imply that the 2 Roseobacteraceae CS4 and Rose1 have the potential for DMSP consumption, while Crocei1 and CS1 might not be able to directly use DMSP.

Nutrient requirements of bacteria were tested in supplementation assays. While CS4 was not affected by amino acid, glucose, DMSP, or vitamin supplements (Fig. 5a), all other bacteria grew better when amino acids and vitamins were supplied (Fig. 5b to d). This growth promotion is less affected by the additional carbon source (Fig. 5). Only a supplement with a carbon source did not promote growth in any of the bacteria.

DISCUSSION

In this study we show that effects of bacteria on phytoplankton manifest already at very low cell counts. In the oceans, nutrients and bacterial cell numbers are low, and thus chemically mediated interactions should be already effective in high dilution. Also, nutrient availability is low in most situations in the plankton and, like in our experiments, bacteria grow slowly (22). In the natural situation, bacteria are also exposed to steep gradients of nutrients when getting into the vicinity of phytoplankton cells. Fast nutrient

TABLE 2 Gene predictions for DMSP metabolism from the genomes of the four bacterial strains, CS4, Rose1, Crocei1, and CS1

| Proteins[a] | Query accession | Gene accession query cover, and identity | | | |
		CS4	Rose1	Crocei1	CS1
DddP	A3SK19.1	WP_219516382.1, 99%, 73.00%	MBW4972570.1, 99%, 80.00%	No	No
DddL	ADK55772.1	WP_219516508.1, 37%, 33.73%	MBW4974109.1, 34%, 32.05%	No	No
DddQ	Q5LT18.1	WP_219513723.1, 28%, 34.48%	MBW4974794.1, 42%, 48.24%	MBW4970188.1, 27%, 32.79%	No
DddW	Q5LW89.1	WP_219516457.1, 80%, 60.66%	No	No	No
DddK	5TG0_A	WP_219516457.1, 66%, 44.44%	No	No	No
	5TFZ_B	WP_219514356.1, 55%, 26.97%			
DddY	E7DDH2.1	No	No	No	No
DddD	A6W2K8.1	WP_219516233.1, 44%, 39.53%	MBW4972965.1, 70%, 26.03%	No	MBW4977114.1, 93%, 23.79%
DddX	7CM9_D	WP_219514187.1, 91%, 25.00%	MBW4973844.1, 91%, 25.63%	No	MBW4980444.1, 89%, 22.25%
DmdA	Q5LS57.1	WP_219514480.1, 96%, 37.82%	MBW4973898.1, 98%, 64.64%	MBW4970937.1, 89%, 26.51%	No
DmdB	Q5LRT0.1	WP_219512577.1, 99%, 47.50%	MBW4975210.1, 99%, 47.22%	MBW4969535.1, 91%, 22.34%	MBW4977128.1, 97%, 36.80%
DmdC	AAV97018.1	WP_219517053.1, 97%, 44.16%	MBW4974836.1, 99%, 40.20%	MBW4969453.1, 62%, 28.23%	MBW4977238.1, 98%, 42.54%
DmdD	AAV97019.1	MBW4983136.1, 93%, 41.27%	MBW4974459.1, 96%, 28.79%	MBW4969944.1, 79%, 35.94%	MBW4978179.1, 70%, 35.60%

[a]The reported DMSP metabolic genes with accession numbers were collected from the previous publications, DddX (57), DddK (58), and the others (59). The bold font shows entries for which the thresholds for coverage and identity are higher than 90% and 35%, respectively.
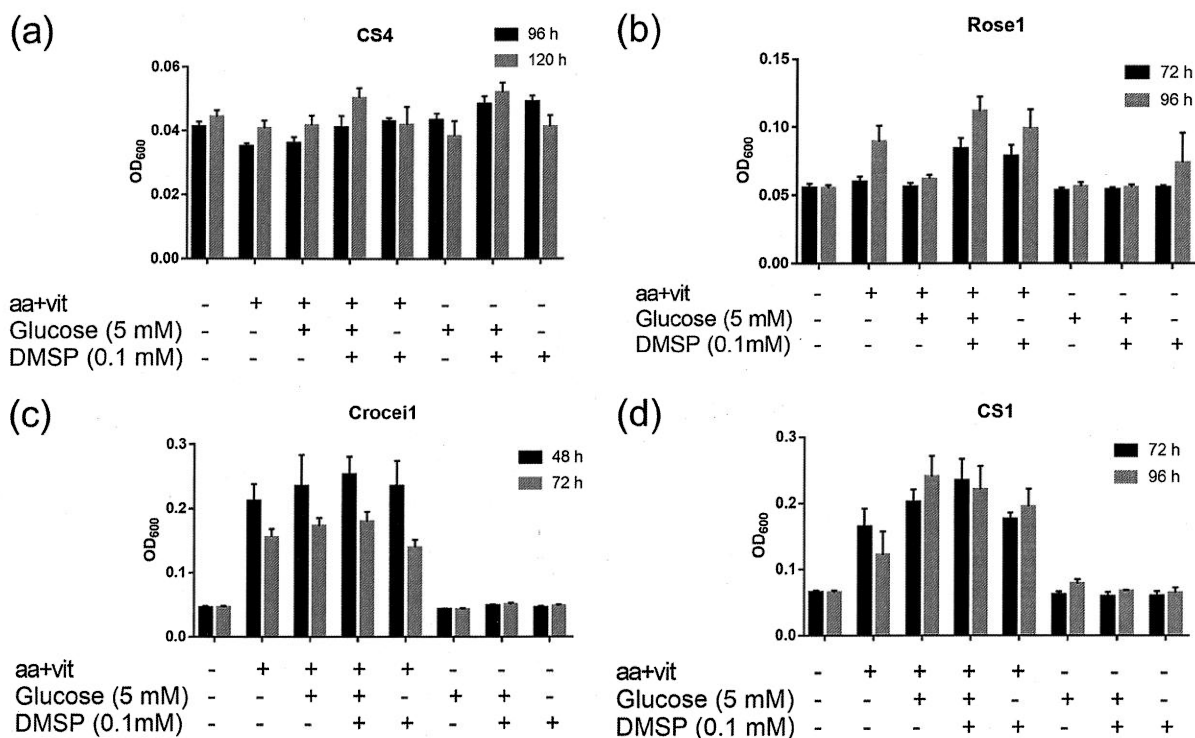
FIG 5 The requirement of the four bacteria (a) CS4, (b) Rose1, (c) Crocei1, and (d) CS1 for nutrients in a minimal medium. The optical density OD_{600} was recorded and used for representing the bacterial growth at an early time point, where first growth was detected by visual inspection (black column) and 24 h later (gray column). Error bars represent the standard deviation of three biological replicates. The statistical analyses of the multiple comparisons are provided in the Table S6.

depletion when resources are consumed or diffused also challenge bacteria in a dynamic way (28). We mimic this short duration of interactions within natural phycospheres situation by transferring bacteria from nutrient enriched media to depleted media (29). In contrast to our set-up, many previous studies on the effect of bacteria on phytoplankton used high optical densities and media optimized for bacterial growth (30). This might be useful for learning about the potential of bacteria to be active but does not account for the fact that certain activities might only be regulated during nutrient depleted situations or under fluctuating environmentally conditions.

The initial survey of pairwise diatom-bacteria interactions revealed that, in most cases, bacteria, even in the low initial cell counts inoculated, influence diatom growth substantially. This high activity might be based on interaction mechanisms that have co-evolved between algae and bacteria. In fact, bacterial communities of diatoms are highly conserved across species and time, which would allow interaction mechanisms to involve (31). We observed growth promotion or inhibition by bacteria depending on the species combinations. Interestingly, we did not identify any universally algicidal or growth-promoting bacteria. In every case, the effect of a given bacterium on algal growth depends on the tested partner. While CS4, for example, inhibits C. socialis, it promotes C. walesii in its growth (Fig. 1b). This species specificity of bacterial effects is in accordance with previous observations of specific algicidal activity in bacteria (32). In our survey, all Gammaproteobacteria inhibited the early stage of C. radiatus growth, while all tested Roseobacteraceae supported the late stage of C. radiatus. This suggests that more general traits like metabolism and substrate usage related to the bacterial phylum might determine these effects (10).

Interaction patterns are further complicated by the observed dependence of bacterial growth modulation on the diatom growth phase. e.g., C. radiatus growth is suppressed by Crocei1 throughout the growth phases, which is consistent with a previous study

(33). In that study, *Croceibacter* was proposed to attach the diatom *Thalassiosira pseudonana* cell and inhibit cell division. The positive effects of Rose 1 and CS4 only occur during the later stages of diatom growth (Fig. 2b and c). These 2 bacteria also decrease the mortality of diatom cells in aged diatom populations (Fig. S13a and b). Such modulating effects might manifest only if the diatoms are already encountering nutrient limited conditions in the stationary phase and are reduced in their fitness. Also, the variable composition of the exo-metabolome of algae, that is highly dependent on the growth phase, can determine the activity of associated bacteria (34). Bacteria might provide essential factors for survival (35). Alternatively, a regulatory switch in bacterial metabolism to support algal survival might be responsible for the observed effects.

The observed interaction between CS1 and *C. radiatus* shows an even more elaborate pattern where the bacterium shifts in its role from an initial growth suppression to later promotion of survival (Fig. 2e). A mechanism can be envisaged where toxins produced by bacteria might inhibit diatom cell division. We also observed that some bacteria promote the growth in the exponential algal growth phase, but are inhibitory in a later phase, or vice versa. Such host fitness-dependent activity shifts have been previously reported in algal-bacteria interactions. They can be caused by a shift of the bacterial metabolism from the release of auxin to the production of algicidal metabolites (36). Variable interaction modes caused by the regulated metabolism of bacteria based on the quorum sensing mediated control of algicidal proteases have also been observed (37). In addition, algae might influence the performance of bacteria. The release of diffusible allelopathic factors, such as polyunsaturated aldehydes or other oxylipins, by the diatom *C. radiatus* might explain the detected bacterial growth inhibition (38). Bacterioplankton development during a diatom bloom in the North Sea can be attributed to algal bloom stages that provide a series of ecological niches for bacteria by producing distinct substrates (39).

Different algae species, or the same species in different physiological states thus form distinctive niches for bacteria, in processes that are likely to be controlled by chemical mediators released from both partners. Related observations on such roles of chemical mediators have been made in synthetic phycospheres (18). They are also indirectly supported through correlations of marine bacterioplankton populations induced by a phytoplankton bloom (29). A special case of chemical mediation is the substrate-based control of interactions, known as resource-based microbial community assembly (29). The algae provide substrates that are required for bacterial growth. In our experiment, the Flavobacterium Crocei1 was fully dependent on the presence of diatom *C. radiatus* (Fig. 3d). From the auxotrophy prediction based on the bacterial genomes, a deficiency in the ability to synthesize amino acids and vitamins in Crocei1 could explain this effect (Table 1). In contrast, *Marinobacter* CS1 that shows fewer deficiencies in its genome compared to Crocei1 also grew well in the absence of diatoms (Fig. 3e).

The microbial model community established in this study is clearly simplified compared to the natural phytoplankton (Fig. 4a and Fig. S16). In nature, a higher diversity of algae and bacteria will be present (40). Nevertheless, our experimental setup represents a situation with a dominant *C. radiatus* bloom and representative bacterial strains from the most prominent clades of the bacterioplankton community (41) that may share the same geographic origin.

Growth suppression of the algae by the bacterial consortium was observed throughout all growth phases (Fig. 2f). The supporting effect of Rose1 and CS4 in the stationary phase did not prevail. All bacteria performed comparably to the pairwise interaction situation. They obviously receive essential substrates, such as amino acids from the algae as can be concluded by their better performance in bilateral diatom/bacteria coculture. Since exposure of phytoplankton to bacteria triggers physiological and metabolic responses, the resulting released metabolites might support fully the growth of the consortium (42). The performance of the bacteria in the consortium with the diatom does not indicate that vitamin production by one community member could overcompensate for the lack of the resource by another. Even vitamin production deficient bacteria

perform similarly in coculture with other bacteria compared to the simple alga/bacteria pairs. This is in accordance with mesocosm experiments that reported increase in phytoplankton and prokaryote biomass associated with vitamin B addition, but no substantial shifts in community composition (43).

Analysis of the substrate utilization capabilities of DMSP suggests that, in our consortium, no bacterial community strategy to support growth mutually can be observed. Based on the genetic inventory, a mechanism could be envisaged where partial DMSP degradation products are exchanged (26, 44). However, such a mechanism does not become obvious, maybe because the algae compensate with the supply of other carbon sources. This is also supported by our observation that the supply of amino acids and vitamins is sufficient to support growth (Fig. 5). Under more limiting conditions, such substrate exchange might become relevant but does not determine the outcome of the community composition in our experiment. In addition, it must be taken into account that bacteria that were in the vicinity of the phycosphere might have repleted storage capacity for nutrients and vitamins that could buffer their responses – a possibility also valid in our experiments where bacteria were transferred between media of different nutrient content (45). Whether these processes hold true for the entire natural plankton community cannot be concluded from our results but can be the subject of future field studies.

We used mathematical modeling to interpret the cell count data from our isolated cultures and cocultures. The growth curves can be nicely explained using a generalized Lotka-Volterra model. It was required that the model takes account of pairwise interactions between alga and bacteria, which can be stimulatory or suppressive and can differ in the early period of growth (1-17 days) compared to the later period (17-41 days). This simple division allowed a good fit, and indicated that the algae might have to be considered as 2 different resources, depending if they do photosynthesis and divide under nutrient repletion or if they rather survive without cell division under limited condition. Such a metabolic shift, according to the growth phase, has been observed for the algal endo metabolome (indicative of their physiology [46]) and the algal exometabolome (indicative of their metabolic interaction [47]). Similar age-dependent algal metabolomes can also be observed during aging blooms in field surveys (48). The strongest pairwise interaction observed is promotion of growth of Crocei1 by the alga, indicating a requirement of the bacterium for essential nutrients or other resources from the alga. Interestingly, the prediction of the growth of the synthetic community containing all 4 bacteria with the alga allowed a quantitatively good agreement with our experimental data by assembling the pairwise interactions. This result hints that pairwise alga-bacteria interactions might be sufficient to explain community dynamics. Such dominance of pairwise-interactions can be observed in nature during the presence of algicidal bacteria that inhibit algal growth (49), but the more subtle interactions of single non-harmful bacteria have, to our knowledge, not been recognized in field surveys. As observed in the coculture, our mathematical modeling suggests that bacteria-bacteria interactions may not be important in this system, since the model recapitulates the data well without including bacteria-bacteria interactions. Similar observations were made in batch cocultures of the dinoflagellate G. catenatum with bacterial communities composed of one-, two-, or three-bacterial partners (50). Bacteria associated with the alga independently modified the growth of the host cell under non-limiting growth conditions, and cocultures exhibited growth curves with a mix of features of the uni bacterial cultures.

To conclude, we observed highly complex interaction patterns between diatoms and associated pelagic bacteria. Our survey documents pronounced species specificity of the interactions. No universal growth-promoting or inhibiting functions of bacteria were observed. Growth phase dependent effects of bacteria on diatoms were common with variable patterns. Fitting our data to a Lotka-Volterra mathematical model confirms that, in simple multipartite communities constructed here, the interaction of the partners decides the outcome of the species composition. Interaction between bacteria,

by, for example, substrate exchange is not determining the community. For natural plankton, this work suggests that species inventories are not sufficient for the prediction of the community development but that more subtle factors, such as algal fitness and regulated bacterial metabolism, have to be taken into account as well.

MATERIALS AND METHODS

Strain selection. Based on the criteria listed in the introduction, we selected 8 widely distributed, ecologically relevant diatoms to screen for growth-promoting or inhibiting effects of bacteria (Fig. 1 and Fig. S1). These included the centric diatoms *C. didymus, C. socialis, Thalassiosira weissflogi, T. nordenskioeldii, C. radiatus, C. wailesii, C. granii,* and a pennate diatom, *Synedra hyperborea.* Among these algae, 6 diatoms were from temperate waters and *T. nordenskioeldii and S. hyperborea* were from the Arctic. *C. socialis* (17), *C. radiatus, C. wailesii,* and *C. granii* (51) originated from Helgoland Roads, North Sea, Germany, where most of the tested bacteria were also isolated (Fig. S1 and Table S1).

Bacteria isolation, identification, and media. The bacterial strains used in this study are listed in Table S2. Except for *Ulvibacter litoralis* 16195 and *Kordia algicida* OT-1, the strains were isolated and identified in this study. For bacterial isolation and purification, 1 mL diatom culture was diluted to 10^{-4}, 10^{-5}, and 10^{-6} fold initial concentration with artificial seawater. One hundred microliter bacterial suspensions in a series of gradient dilutions were poured and spread on Marine Broth (MB) agar plates. After incubation for 3 to 6 days at 28°C, single colonies were picked and transferred to a new MB agar plate using autoclaved toothpicks by plate scribing. The above steps were repeated two times to obtain pure cultures. New single colonies were transferred into 3 mL liquid MB medium in 10 mL sterile tubes and cultured at 28°C under shaking 150 rpm. When the OD_{600} reached 0.5 to 0.8, 1 mL of the bacterial cultures were harvested in 1.5 mL Eppendorf tubes and collected by centrifugation at 12 000 rpm for 1 min at room temperature. The resulting cell pellet was used for DNA extraction with a Quick-DNA Fungal/Bacterial Miniprep Kit (ZYMO RESEARCH) following the manufacturer's protocol. One microliter properly diluted DNA sample was added as the template to 20 μL PCR solution with 1.25 U DreamTaq DNA polymerase (Thermo Scientific). The 16S rRNA gene was amplified with the universe primers 27F (5'-AGAGTTTGATCCTGGCTCAG-3') and 1492R (5'-ACGGHTACCTTGTTACGACTT-3') under the conditions: 5 min at 95°C, 30 cycles of 30 s at 95°C, 30 s at 55°C and 90 s at 72°C, another 10 min at 72°C for extension, and paused at 24°C. The PCR products were verified by agarose gel electrophoresis for quality control. The PCR products were sent to Eurofins Genomics (Eurofins Genomics, Ebersberg, Germany) for sequencing. The sequencing results of these isolates were used to construct a phylogenetic tree based on maximum likelihood using the software MEGAX version 10.1.7.

The media for diatom cultivation and co-cultivation used in this study are listed in Table S1. All media were made from artificial seawater (52) buffered with 5 mM HEPES. For ASW1 medium, extra trace element solution was added with the final concentrations of 80 pM $Na_2EDTA \cdot 2H_2O$, 25 pM $(NH_4)_2Fe(II)(SO_4)_2 \cdot 6H_2O$, 100 pM H_3BO_3, 10 pM $MnCl_2 \cdot 4H_2O$, 10 pM $ZnCl_2$, 2 pM $Na_2MoO_4 \cdot 2H_2O$, 0.1 pM $CuSO_4 \cdot 5H_2O$, 0.1 pM $CoCl_2 \cdot 6H_2O$, 0.1 pM $NaVO_3$, 10 nM $Na_2SeO_3 \cdot 5H_2O$. For ASW2 medium, extra 50 times f/2 stock solution (Sigma G9903) and additional silicate was added to the final concentration of 400 μM to optimize the growth of *Coscinodiscus* strains. For ASW3 medium, extra 1 mL $NaNO_3$ (75.0 g/L dH_2O), 1 mL $NaH_2PO_4 \cdot H_2O$ (5.0 g/L dH_2O), 1 mL $Na_2SiO_3 \cdot 9H_2O$ (30.0 g/L dH_2O), 1 mL L1 trace metal solution and 0.5 mL f/2 vitamin solution (53) were supplemented. The diatom cultures were incubated at 13°C with a diurnal rhythm of light: dark cycle of 15 h: 9 h and light intensity of 25 $\mu mol \times m^{-2} \times s^{-1}$.

Bacteria-diatom co-cultivation. Diatoms were purified to reduce the bacterial level using a protocol for the generation of axenic cultures (54) with the following modifications. In total, 20 mL culture from exponential phase for each diatom culture was filtered with polycarbonate membranes (pluriSelect Life Science), 5 μm for *C. socialis, C. didymus, C. granii, T. weissflogii, T. nordenskioeldii,* and *S. hyperborea,* 40 μm for *C. radiatus, C. wailesii.* Then, the diatom cells on the filters were washed with 10 mL final concentration of 20 μg/mL Triton X-100 in the corresponding medium to remove attached bacteria, and afterward with 10 mL fresh medium to remove Triton X-100. The antibiotic ciprofloxacin was added to the cultures at a final concentration of 10 μg/mL. After incubation of these diatom cultures under the conditions mentioned above for 24 h, the antibiotic was removed by another filtration and taken up in fresh medium. The diatom cultures (300 μL) were distributed in 48-well plates with appropriate initial concentrations.

Each bacterial inoculum was prepared from a fresh MB culture (3 mL). The conditions for cultivation are as described above for bacterial DNA extraction. When the OD_{600} of bacterial cultures reached 0.5 to 0.8, the bacterial cultures were harvested in 1.5 mL sterile Eppendorf tubes by centrifugation at 12 000 rpm for 1 min at room temperature. Bacterial cell pellets were washed two times with 1 mL artificial seawater to completely remove MB. The bacterial inoculum was inoculated to the diatom cultures to give an initial concentration of 10^5-10^6 cells/mL. Diatom cultures without bacterial inoculation were used as controls. Each treatment was replicated three times. The 48-well plates were covered with gas-permeable membranes and incubated at 13°C under a gentle shaking of 40 rpm with a diurnal rhythm of light: dark cycle of 15 h: 9 h and light intensity of 25 $\mu mol \times m^{-2} \times s^{-1}$.

To investigate the interaction of *C. radiatus* with the bacterial community of 4 species, more intensive antibiotics treatment with 50 μg/mL kanamycin and 20 μg/mL ciprofloxacin was applied for 24 h to purify the cultures. The initial axenic state was monitored by plate spreading. The *C. radiatus* culture was inoculated with a final density of 3 cells/mL into tissue culture flasks (TC Flask T75, Sarstedt) containing 150 mL ASW2 medium. The bacteria CS4, Rose, Crocei1, and CS1 were inoculated with the final density

of 10^3-10^4 cells/mL for co-cultivation under the conditions mentioned above. No shaking was applied in this case. Three biological replicates were set for each group.

Chl, a measurement and calculation of interactive effects. Chl a was measured using a Varioskan Flash Multimode Reader (Thermo Fisher Scientific) with the following parameters: The 48-well plate was shaken with the speed of 300 rpm and diameter 5 mm for 20 s and then stopped for 50 s before measurement. For Chl a fluorescence detection, the excitation wavelength is 430 nm with a bandwidth of 12 nm and the emission wavelength was set as 665 nm. The acquisition mode was set as "read from plate bottom". The measurement time was 100 ms. Multipoint mode was used with a safety zone 1.4 mm. Chl a was measured every other day.

We selected the proper time points for each diatom to represent the corresponding early and late phases based on the chlorophyll reads and, for each time point, the rations of Chl a values between the growth of diatom inoculated with and without bacteria were calculated. An exception is the diatom *S. hyperborea* RCC5218. This strain originated from cold seawater and did not show growth at 13°C after the bacterial community had been reduced. Thus, the effects of different bacteria on the growth of *S. hyperborea* were calculated via normalization of the growth with its average Chl a value. After logarithmic transformation of the ratios with base 2, the corresponding values were used for generating the heat map.

***C. radiatus* cell counting.** *C. radiatus* growth was monitored by cell counting. After thorough shaking and mixing the culture, the volume of 300 μL sample was transferred to a 48-well plate and was observed under a Leica DM2500 microscope equipped with a CCD system, and the software NIC-elements D 4.30.00 was used for documentation by photography. Live cells and dead cells were recorded as shown in Fig. S11.

Bacterial quantification by qPCR. The primers for specific amplification of the 4 strains, CS4, Rose1, Cro1, and CS1 were designed based on their 16S rRNA gene sequences after running the multiple-sequence alignments via the software MEGA (version 10.1.7). Designed primers were further tested using the online tool testprime on https://www.arb-silva.de/search/testprime. Primers were synthesized by the company Biomers,) and are listed in Table S3. Primer efficiency for qPCR for all bacterial strains and primer specificity among the 4 strains were tested.

For qPCR analysis, 1 mL coculture sample was transferred to a 1.5 mL Eppendorf tube for a simple and rapid method for genome DNA preparation based on a previously reported protocol (55) with minor modifications. Briefly, we harvested the cell pellet by centrifugation at 13 000 rpm for 20 min. After removing the supernatant, 100 μL TE buffer (10 mM Tris and 1 mM EDTA, pH 8.0) was added to resuspend the cell pellet. Then, the samples were heated to 100°C for 10 min with 200 rpm shaking. After heating, the samples were transferred on ice for 10 min. Finally, the samples were centrifuged at 13 000 rpm at 4°C for 15 min. After centrifugation, 0.5 μL of supernatant was added to a 10 μL qPCR system containing 5 μL PowerUp SYBR Green Master Mix (Thermo Fisher Scientific), 1 μL of the forward and reverse premixed primers with the final concentration of 0.5 μM for each, and 3.5 μL of distilled water. Standard cycling mode was used for qPCR procedure with following steps: UDG activation at 50°C for 2 min, polymerase activation at 95°C for 2 min, 40 cycles to denature at 95°C for 15 s, anneal at 55°C for 15 s, and extend at 72°C for 1 min.

For calibration, the Cq values from qPCR with the bacterial cells/mL, we prepared 2 mL of a series of 10 times gradient dilution of the 4 bacterial suspensions. 1 mL suspension was used for pouring MB agar plate and bacterial colonies counting. Another 1 mL suspension was used to prepare DNA samples for the qPCR as the steps mentioned above.

Interpretation of bacteria-diatom pairwise interactions with a generalized Lotka-Volterra model. Our mathematical model consists of the following set of differential equations (see Materials and Methods for details):

$$\frac{dS_1}{dt} = \mu_1 S_1 \left(1 + a_{11}\frac{S_1}{K+S_1} + a_{12}S_2 + a_{13}S_3 + a_{14}S_4 + a_{15}S_5 \right)$$

$$\frac{dS_2}{dt} = \mu_2 S_2 (1 + a_{21}S_1 + a_{22}S_2)$$

$$\frac{dS_3}{dt} = \mu_3 S_3 (1 + a_{31}S_1 + a_{33}S_3)$$

$$\frac{dS_4}{dt} = \mu_4 S_4 (1 + a_{41}S_1 + a_{44}S_4)$$

$$\frac{dS_5}{dt} = \mu_5 S_5 (1 + a_{51}S_1 + a_{55}S_5)$$

(1)

Here, S_1 represents the cell density (number of individuals per volume) of the diatom, and S_2...S_5 represent the cell densities of the bacteria CS4, Rose1, Creocei1, and CS1, respectively. In the monocultures, the parameters μ_1, a_{11}, and K describe the growth of the diatom *C. radiatus*, μ_2 and a_{22} describe the growth of CS4, μ_3 and a_{33} the growth of Rose1, μ_4 and a_{44} Creocei1, and μ_5 and a_{55} CS1 (see Materials and Methods). The remaining parameters, a_{21}, a_{31}, etc. describe the pairwise interactions between the diatom and each bacterium. A key aspect of the Lotka-Volterra model is to predict the behavior of the synthetic community from the pairwise alga-bacterium cultivation.

To interpret the data from cocultures, we first fitted the Lotka-Volterra model (Equations 1 to the cell count data for the alga and each bacterium in isolation, to obtaining parameters μ_1, a_{11}, K, μ_2... μ_5 and a_{22}... a_{55}. Next, we fitted the model to the pairwise coculture data to obtain the remaining parameters (Fig. S14 and Fig. S15). To perform these fits, we split the data into 2 separate time periods, 1-17 days and 17–41 days, since the algal growth dynamics is qualitatively different in these 2 phases. Indeed, the

algal cell counts increased during days 1–17 and decreased during days 17–41. We, therefore, obtained 2 sets of model parameters describing these 2 time periods (Fig. 4a and Table S4). Finally, we used the mathematical model to predict the growth of the synthetic model community with the four bacteria, as shown in Fig. 2. Further details are given in the Supporting Information.

Bacterial genome sequencing and mining. Bacterial DNA was extracted by Quick-DNA Fungal/Bacterial Miniprep (ZYMO RESEARCH) as described above. DNA concentration was measured in a Qubit 3.0 Fluorometer (Invitrogen). The DNA samples concentrations for the four strains, CS4, Rose1, Crocei1, and CS1 are 17 ng/μL, 55 ng/μL, 8 ng/μL, 30 ng/μL, respectively, in 100 μL TE buffer. The qualified samples were sent to Eurofins Genomics (Konstanz, Germany) and were sequenced by the sequencing technology Illumina HiSeq on the NovaSeq 6000 sequencing system platform. The sequencing was performed with the flow cell type S2, the configuration PE150, and XP workflow. We released the whole genome sequences of these bacteria to the NCBI genome database under the BioProject accession PRJNA748384. The basic genomic sequence information of the 4 strains are shown in Table S5. The closest match that represents their taxonomic status was analyzed via Kbase SpeciesTree v2.2.0 app based on the genome sequences (version 2.3.2 of KBase UI, https://www.kbase.us/). The auxotrophy prediction for the 4 bacterial genomes was applied using an integrated app of Predict Genome Auxotrophies v2.0.0 in Kbase. Those collected protein sequences were used as query sequences to search against the 4 bacterial genomes via BLASTP.

Bacterial nutrient requirement analysis. For bacterial nutrient requirement analysis, 3 groups of nutrients were added into minimal basal medium (MBM) (56) in different combinations. The group 1 supplement contained 0.1 mM DMSP (Sigma-Aldrich), the group 2 supplement contained 5 mM glucose, and the group 3 supplements contained 13 amino acids, including l-glutamate, glycine, L-alanine, L-aspartate, L-arginine, L-glutamine, L-serine, L-tyrosine, L-leucine, L-proline, L-valine, L-threonine, and L-isoleucine each with 0.3 mM as the final concentration together with a previously reported vitamin solution for MBM (56). Bacterial inoculum was prepared the same way as previously mentioned for co-cultivation experiment. After washing twice to remove MB medium and resuspending in minimal medium with OD_{600} = 0.2, the volume of 30 μL bacterial suspension was inoculated into 3 mL minimal medium with different combinations of nutrients groups in 10 mL sterile tubes and cultivated in 28°C incubator with 150 rpm shaking. The volume of 0.5 mL culture was taken and transferred into 1 cm cuvettes for OD_{600} measurement by spectrophotometer during 2–5 days after the inoculation. Three replicates were set for each treatment.

Data availability. The accession numbers for the partial 16s rRNA gene nucleotide sequences were deposited in the NCBI as listed in Table S2. The genome sequences were released to the NCBI genome database under the BioProject accession PRJNA748384. Individual genome accessions are listed in Table S5.

SUPPLEMENTAL MATERIAL

Supplemental material is available online only.
SUPPLEMENTAL FILE 1, PDF file, 3.1 MB.

ACKNOWLEDGMENTS

REFERENCES

1. Khangaonkar T, Sackmann B, Long W, Mohamedali T, Roberts M. 2012. Simulation of annual biogeochemical cycles of nutrient balance, phytoplankton bloom(s), and DO in Puget Sound using an unstructured grid model. Ocean Dynamics 62:1353–1379. https://doi.org/10.1007/s10236-012-0562-4.

2. Needham DM, Fuhrman JA. 2016. Pronounced daily succession of phytoplankton, archaea and bacteria following a spring bloom. Nat Microbiol 1:16005. https://doi.org/10.1038/nmicrobiol.2016.5.

3. Schleyer G, Vardi A. 2020. Algal blooms. Curr Biol 30:R1116–R1118. https://doi.org/10.1016/j.cub.2020.07.011.

4. Deng Y, Vallet M, Pohnert G. 2022. Temporal and spatial signaling mediating the balance of the plankton microbiome. Annu Rev Mar Sci 14:239–260. https://doi.org/10.1146/annurev-marine-042021-012353.

5. Litchman E, Klausmeier CA. 2008. Trait-based community ecology of phytoplankton. Annu Rev Ecol Evol Syst 39:615–639. https://doi.org/10.1146/annurev.ecolsys.39.110707.173549.

6. Vardi A. 2008. Cell signaling in marine diatoms. Commun Integr Biol 1:134–136. https://doi.org/10.4161/cib.1.2.6867.

7. Bidle KD. 2016. Programmed cell death in unicellular phytoplankton. Curr Biol 26:R594–R607. https://doi.org/10.1016/j.cub.2016.05.056.

8. Vardi A, Formiggini F, Casotti R, De Martino A, Ribalet F, Miralto A, Bowler C. 2006. A stress surveillance system based on calcium and nitric oxide in marine diatoms. PLoS Biol 4:e60. https://doi.org/10.1371/journal.pbio.0040060.

9. Nelson DM, Treguer P, Brzezinski MA, Leynaert A, Queguiner B. 1995. Production and dissolution of biogenic silica in the ocean - revised global estimates, comparison with regional data and relationship to biogenic sedimentation. Global Biogeochem Cycles 9:359–372. https://doi.org/10.1029/95GB01070.

10. Buchan A, LeCleir GR, Gulvik CA, Gonzalez JM. 2014. Master recyclers: features and functions of bacteria associated with phytoplankton blooms. Nat Rev Microbiol 12:686–698. https://doi.org/10.1038/nrmicro3326.

11. Amin SA, Hmelo LR, van Tol HM, Durham BP, Carlson LT, Heal KR, Morales RL, Berthiaume CT, Parker MS, Djunaedi B, Ingalls AE, Parsek MR, Moran MA, Armbrust EV. 2015. Interaction and signalling between a cosmopolitan phytoplankton and associated bacteria. Nature 522:98–101. https://doi.org/10.1038/nature14488.

12. Sonnenschein EC, Syit DA, Grossart HP, Ullrich MS. 2012. Chemotaxis of *Marinobacter adhaerens* and its impact on attachment to the diatom *Thalassiosira weissflogii*. Appl Environ Microbiol 78:6900–6907. https://doi.org/10.1128/AEM.01790-12.

13. Barak-Gavish N, Frada MJ, Ku C, Lee PA, DiTullio GR, Malitsky S, Aharoni A, Green SJ, Rotkopf R, Kartvelishvily E, Sheyn U, Schatz D, Vardi A. 2018.

Bacterial virulence against an oceanic bloom-forming phytoplankter is mediated by algal. DMSP Sci Adv 4:eaau5716. https://doi.org/10.1126/sciadv.aau5716.

14. Bigalke A, Pohnert G. 2019. Algicidal bacteria trigger contrasting responses in model diatom communities of different composition. Microbiologyopen 8:e00818. https://doi.org/10.1002/mbo3.818.

15. Seymour JR, Amin SA, Raina JB, Stocker R. 2017. Zooming in on the phycosphere: the ecological interface for phytoplankton-bacteria relationships. Nat Microbiol 2:17065. https://doi.org/10.1038/nmicrobiol.2017.65.

16. Amin SA, Parker MS, Armbrust EV. 2012. Interactions between diatoms and bacteria. Microbiol Mol Biol Rev 76:667–684. https://doi.org/10.1128/MMBR.00007-12.

17. Bigalke A, Meyer N, Papanikolopoulou LA, Wiltshire KH, Pohnert G. 2019. The algicidal bacterium *Kordia algicida* shapes a natural plankton community. Appl Environ Microbiol 85:e02779-18. https://doi.org/10.1128/AEM.02779-18.

18. Kim H, Kimbrel JA, Vaiana CA, Wollard JR, Mayali X, Buie CR. 2022. Bacterial response to spatial gradients of algal-derived nutrients in a porous microplate. ISME J 16:1036–1045. https://doi.org/10.1038/s41396-021-01147-x.

19. Liang KYH, Orata FD, Boucher YF, Case RJ. 2021. Roseobacters in a sea of poly- and paraphyly: whole genome-based taxonomy of the family Rhodobacteraceae and the proposal for the split of the "Roseobacter Clade" Into a novel family, Roseobacteraceae fam. nov. Front Microbiol 12:683109. https://doi.org/10.3389/fmicb.2021.683109.

20. Sunagawa S, Coelho LP, Chaffron S, Kultima JR, Labadie K, Salazar G, Djahanschiri B, Zeller G, Mende DR, Alberti A, Cornejo-Castillo FM, Costea PI, Cruaud C, d'Ovidio F, Engelen S, Ferrera I, Gasol JM, Guidi L, Hildebrand F, Kokoszka F, Lepoivre C, Lima-Mendez G, Poulain J, Poulos BT, Royo-Llonch M, Sarmento H, Vieira-Silva S, Dimier C, Picheral M, Searson S, Kandels-Lewis S, Bowler C, de Vargas C, Gorsky G, Grimsley N, Hingamp P, Iudicone D, Jaillon O, Not F, Ogata H, Pesant S, Speich S, Stemmann L, Sullivan MB, Weissenbach J, Wincker P, Karsenti E, Raes J, Acinas SG, Bork P, Tara Oceans coordinators. 2015. Ocean plankton. Structure and function of the global ocean microbiome. Science 348:1261359. https://doi.org/10.1126/science.1261359.

21. Vallet M, Baumeister TUH, Kaftan F, Grabe V, Buaya A, Thines M, Svatos A, Pohnert G. 2019. The oomycete *Lagenisma coscinodisci* hijacks host alkaloid synthesis during infection of a marine diatom. Nat Commun 10:4938. https://doi.org/10.1038/s41467-019-12908-w.

22. Whitman WB, Coleman DC, Wiebe WJ. 1998. Prokaryotes: the unseen majority. Proc Natl Acad Sci U S A 95:6578–6583. https://doi.org/10.1073/pnas.95.12.6578.

23. Momeni B, Xie L, Shou W. 2017. Lotka-Volterra pairwise modeling fails to capture diverse pairwise microbial interactions. Elife 6:e25051. https://doi.org/10.7554/eLife.25051.

24. Volterra V. 1928. Variations and fluctuations of the number of individuals in animal species living together. ICES J Marine Science 3:3–51. https://doi.org/10.1093/icesjms/3.1.3.

25. Johnson WM, Alexander H, Bier RL, Miller DR, Muscarella ME, Pitz KJ, Smith H. 2020. Auxotrophic interactions: a stabilizing attribute of aquatic microbial communities? FEMS Microbiol Ecol 96:fiaa115. https://doi.org/10.1093/femsec/fiaa115.

26. Curson AR, Todd JD, Sullivan MJ, Johnston AW. 2011. Catabolism of dimethylsulphoniopropionate: microorganisms, enzymes and genes. Nat Rev Microbiol 9:849–859. https://doi.org/10.1038/nrmicro2653.

27. Shaw DK, Sekar J, Ramalingam PV. 2022. Recent insights into oceanic dimethylsulfoniopropionate biosynthesis and catabolism. Environ Microbiol 24:2669–2700. https://doi.org/10.1111/1462-2920.16045.

28. Gao C, Fernandez VI, Lee KS, Fenizia S, Pohnert G, Seymour JR, Raina JB, Stocker R. 2020. Single-cell bacterial transcription measurements reveal the importance of dimethylsulfoniopropionate (DMSP) hotspots in ocean sulfur cycling. Nat Commun 11:1942. https://doi.org/10.1038/s41467-020-15693-z.

29. Fu H, Uchimiya M, Gore J, Moran MA. 2020. Ecological drivers of bacterial community assembly in synthetic phycospheres. Proc Natl Acad Sci U S A 117:3656–3662. https://doi.org/10.1073/pnas.1917265117.

30. Cirri E, Pohnert G. 2019. Algae−bacteria interactions that balance the planktonic microbiome. New Phytol 223:100–106. https://doi.org/10.1111/nph.15765.

31. Behringer G, Ochsenkuhn MA, Fei C, Fanning J, Koester JA, Amin SA. 2018. Bacterial communities of diatoms display strong conservation across strains and time. Front Microbiol 9:e659. https://doi.org/10.3389/fmicb.2018.00659.

32. Zhang F, Ye Q, Chen Q, Yang K, Zhang D, Chen Z, Lu S, Shao X, Fan Y, Yao L, Ke L, Zheng T, Xu H. 2018. Algicidal activity of novel marine bacterium *Paracoccus* sp. strain Y42 against a harmful algal-bloom-causing dinoflagellate, *Prorocentrum donghaiense*. Appl Environ Microbiol 84:e01015-18. https://doi.org/10.1128/AEM.01015-18.

33. van Tol HM, Amin SA, Armbrust EV. 2017. Ubiquitous marine bacterium inhibits diatom cell division. ISME J 11:31–42. https://doi.org/10.1038/ismej.2016.112.

34. Olofsson M, Ferrer-González FX, Uchimiya M, Schreier JE, Holderman NR, Smith CB, Edison AS, Moran MA. 2022. Growth-stage-related shifts in diatom endometabolome composition set the stage for bacterial heterotrophy. ISME Commun 2:28. https://doi.org/10.1038/s43705-022-00116-5.

35. Droop MR. 2007. Vitamins, phytoplankton and bacteria: symbiosis or scavenging? J Plankton Res 29:107–113. https://doi.org/10.1093/plankt/fbm009.

36. Seyedsayamdost MR, Case RJ, Kolter R, Clardy J. 2011. The Jekyll-and-Hyde chemistry of Phaeobacter gallaeciensis. Nat Chem 3:331–335. https://doi.org/10.1038/nchem.1002.

37. Paul C, Pohnert G. 2011. Interactions of the algicidal bacterium *Kordia algicida* with diatoms: regulated protease excretion for specific algal lysis. PLoS One 6:e21032. https://doi.org/10.1371/journal.pone.0021032.

38. Edwards BR, Bidle KD, Van Mooy BA. 2015. Dose-dependent regulation of microbial activity on sinking particles by polyunsaturated aldehydes: Implications for the carbon cycle. Proc Natl Acad Sci U S A 112:5909–5914. https://doi.org/10.1073/pnas.1422664112.

39. Teeling H, Fuchs BM, Becher D, Klockow C, Gardebrecht A, Bennke CM, Kassabgy M, Huang SX, Mann AJ, Waldmann J, Weber M, Klindworth A, Otto A, Lange J, Bernhardt J, Reinsch C, Hecker M, Peplies J, Bockelmann FD, Callies U, Gerdts G, Wichels A, Wiltshire KH, Glockner FO, Schweder T, Amann R. 2012. Substrate-controlled succession of marine bacterioplankton populations induced by a phytoplankton bloom. Science 336:608–611. https://doi.org/10.1126/science.1218344.

40. Sunagawa S, Acinas SG, Bork P, Bowler C, Eveillard D, Gorsky G, Guidi L, Iudicone D, Karsenti E, Lombard F, Ogata H, Pesant S, Sullivan MB, Wincker P, de Vargas C, Tara Oceans C. 2020. Tara Oceans: towards global ocean ecosystems biology. Nat Rev Microbiol 18:428–445. https://doi.org/10.1038/s41579-020-0364-5.

41. Teeling H, Fuchs BM, Bennke CM, Kruger K, Chafee M, Kappelmann L, Reintjes G, Waldmann J, Quast C, Glockner FO, Lucas J, Wichels A, Gerdts G, Wiltshire KH, Amann RI. 2016. Recurring patterns in bacterioplankton dynamics during coastal spring algae blooms. Elife 5:e11888. https://doi.org/10.7554/eLife.11888.

42. Shibl AA, Isaac A, Ochsenkuhn MA, Cardenas A, Fei C, Behringer G, Arnoux M, Drou N, Santos MP, Gunsalus KC, Voolstra CR, Amin SA. 2020. Diatom modulation of select bacteria through use of two unique secondary metabolites. Proc Natl Acad Sci U S A 117:27445–27455. https://doi.org/10.1073/pnas.2012088117.

43. Joglar V, Pontiller B, Martinez-Garcia S, Fuentes-Lema A, Perez-Lorenzo M, Lundin D, Pinhassi J, Fernandez E, Teira E. 2021. Microbial plankton community structure and function responses to vitamin B-12 and B-1 amendments in an upwelling system. Appl Environ Microbiol 87:e01525-21. https://doi.org/10.1128/AEM.01525-21.

44. Bullock HA, Luo HW, Whitman WB. 2017. Evolution of dimethylsulfoniopropionate metabolism in marine phytoplankton and bacteria. Front Microbiol 8:637. https://doi.org/10.3389/fmicb.2017.00637.

45. Daly G, Ghini V, Adessi A, Fondi M, Buchan A, Viti C. 2022. Towards a mechanistic understanding of microalgae-bacteria interactions: integration of metabolomic analysis and computational models. FEMS Microbiology Rev 46:fuac020. https://doi.org/10.1093/femsre/fuac020.

46. Vidoudez C, Pohnert G. 2012. Comparative metabolomics of the diatom *Skeletonema marinoi* in different growth phases. Metabolomics 8:654–669. https://doi.org/10.1007/s11306-011-0356-6.

47. Barofsky A, Vidoudez C, Pohnert G. 2009. Metabolic profiling reveals growth stage variability in diatom exudates. Limnol Oceanogr Methods 7:382–390. https://doi.org/10.4319/lom.2009.7.382.

48. Kuhlisch C, Althammer J, Sazhin AF, Jakobsen HH, Nejstgaard JC, Pohnert G. 2020. Metabolomics-derived marker metabolites to characterize *Phaeocystis pouchetii* physiology in natural plankton communities. Sci Rep 10:20444. https://doi.org/10.1038/s41598-020-77169-w.

49. Sohn JH, Lee JH, Yi H, Chun J, Bae KS, Ahn TY, Kim SJ. 2004. Kordia algicida gen. nov., sp nov., an algicidal bacterium isolated from red tide. Int J Syst Evol Microbiol 54:675–680. https://doi.org/10.1099/ijs.0.02689-0.

50. Bolch CJS, Bejoy TA, Green DH. 2017. Bacterial associates modify growth dynamics of the dinoflagellate *Gymnodinium catenatum*. Front Microbiol 8:670. https://doi.org/10.3389/fmicb.2017.00670.

51. Buaya A, Kraberg A, Thines M. 2019. Dual culture of the oomycete *Lagenisma coscinodisci* Drebes and *Coscinodiscus* diatoms as a model for

plankton/parasite interactions. Helgol Mar Res 73:2. https://doi.org/10.1186/s10152-019-0523-0.

52. Maier I, Calenberg M. 1994. Effect of extracellular Ca²⁺ and Ca²⁺-antagonists on the movement and chemoorientation of male gametes of *Ectocarpus siliculosus* (Phaeophyceae). Botanica Acta 107:451–460. https://doi.org/10.1111/j.1438-8677.1994.tb00820.x.

53. Guillard RRL. 1975. Culture of phytoplankton for feeding marine invertebrates, p 29–60. *In* Smith WL, Chanley MH (ed), Culture of marine invertebrate animals: Proceedings — 1st conference on culture of marine invertebrate animals greenport. Springer US, Boston, MA.

54. Shishlyannikov SM, Zakharova YR, Volokitina NA, Mikhailov IS, Petrova DP, Likhoshway YV. 2011. A procedure for establishing an axenic culture of the diatom *Synedra acus* subsp *radians* (Kutz.) Skabibitsch from Lake Baikal. Limnol Oceanogr Methods 9:478–484. https://doi.org/10.4319/lom.2011.9.478.

55. Edwards K, Johnstone C, Thompson C. 1991. A simple and rapid method for the preparation of plant genomic DNA for PCR analysis. Nucleic Acids Res 19:1349. https://doi.org/10.1093/nar/19.6.1349.

56. Gonzalez JM, Mayer F, Moran MA, Hodson RE, Whitman WB. 1997. *Microbulbifer hydrolyticus* gen. nov., sp. nov., and *Marinobacterium georgiense* gen. nov., sp. nov., two marine bacteria from a lignin-rich pulp mill waste enrichment community. Int J Syst Bacteriol 47:369–376. https://doi.org/10.1099/00207713-47-2-369.

57. Li CY, Wang XJ, Chen XL, Sheng Q, Zhang S, Wang P, Quareshy M, Rihtman B, Shao X, Gao C, Li FC, Li SY, Zhang WP, Zhang XH, Yang GP, Todd JD, Chen Y, Zhang YZ. 2021. A novel ATP dependent dimethylsulfoniopropionate lyase in bacteria that releases dimethyl sulfide and acryloyl-CoA. Elife 10:e64045. https://doi.org/10.7554/eLife.64045.

58. Sun J, Todd JD, Thrash JC, Qian YP, Qian MC, Temperton B, Guo JZ, Fowler EK, Aldrich JT, Nicora CD, Lipton MS, Smith RD, De Leenheer P, Payne SH, Johnston AWB, Davie-Martin CL, Halsey KH, Giovannoni SJ. 2016. The abundant marine bacterium Pelagibacter simultaneously catabolizes dimethylsulfoniopropionate to the gases dimethyl sulfide and methanethiol. Nat Microbiol 1:16065. https://doi.org/10.1038/nmicrobiol.2016.65.

59. Reisch CR, Moran MA, Whitman WB. 2011. Bacterial catabolism of dimethylsulfoniopropionate (DMSP). Front Microbiol 2:172. https://doi.org/10.3389/fmicb.2011.00172.